



**Mediating covalent crosslinking of single-chain nanoparticles through solvophobicity in organic solvents**

Journal:	<i>Polymer Chemistry</i>
Manuscript ID	PY-COM-06-2021-000780.R1
Article Type:	Communication
Date Submitted by the Author:	15-Jul-2021
Complete List of Authors:	<p>Scheutz, Georg; University of Florida, Department of Chemistry          Elgoyhen, Justine; University of Florida, Department of Chemistry          Bentz, Kyle; University of California, San Diego, Dept. of Chemistry and Biochemistry          Xia, Yening; South China University of Technology, Faculty of Materials Science and Engineering          Sun, Hao; northwestern university, Chemistry          Zhao, Junpeng; South China University of Technology, Faculty of Materials Science and Engineering          Savin, Daniel; University of Florida, Chemistry          Sumerlin, Brent; University of Florida, Department of Chemistry;</p>

## COMMUNICATION

## Mediating covalent crosslinking of single-chain nanoparticles through solvophobicity in organic solvents

Received 00th January 20xx,  
Accepted 00th January 20xx

Georg M. Scheutz,<sup>a</sup> Justine Elgoyhen,<sup>a</sup> Kyle C. Bentz,<sup>a</sup> Yening Xia,<sup>a,b</sup> Hao Sun,<sup>a</sup> Junpeng Zhao,<sup>b</sup> Daniel A. Savin<sup>a</sup> and Brent S. Sumerlin<sup>\*a</sup>

DOI: 10.1039/x0xx00000x

We describe the photoinduced intrachain crosslinking of coumarin-containing copolymers in various organic solvents. Analysis of copolymer solvation and comparison to a molecular coumarin derivative revealed solvophobicity-driven crosslinking kinetics and chain compaction that facilitated the synthesis of single-chain nanoparticles.

Intramolecular crosslinking of single polymer chains affords single-chain nanoparticles (SCNPs).<sup>1</sup> Similar to biomacromolecules that acquire form and function from a precise chain folding process, the compaction of linear polymer chains has provided nanoparticles with promising performances in areas such as catalysis,<sup>2-5</sup> cargo delivery,<sup>6-8</sup> or advanced materials.<sup>9-12</sup> Control over the crosslinking reaction kinetics has proven critical for the successful formation of such SCNPs.<sup>13-16</sup> Here, we demonstrate the potential of the solvophobic effect in organic solvents to mediate the crosslinking of linear polymers into SCNPs.

Despite their promise as well-defined nanomaterials, preparation of SCNPs is complicated by the requirement of high dilution to favor intramolecular crosslinking over intermolecular reactions. One effective strategy to direct SCNP formation relies on intramolecular collapse of amphiphilic polymers in water prior to covalent crosslinking.<sup>17,18</sup> However, formation of more hydrophobic SCNPs necessitates the use of organic solvent systems during synthesis and processing. Corroborating computational predictions,<sup>19-21</sup> the groups of Simon<sup>22</sup> and Lederer<sup>23</sup> have observed that crosslinking under poor solvent conditions promotes higher reaction conversions and more compacted SCNPs.<sup>22,23</sup> Among other factors, this phenomenon was primarily attributed to decreased polymer chain solvation and reduced chain dimensions in poor

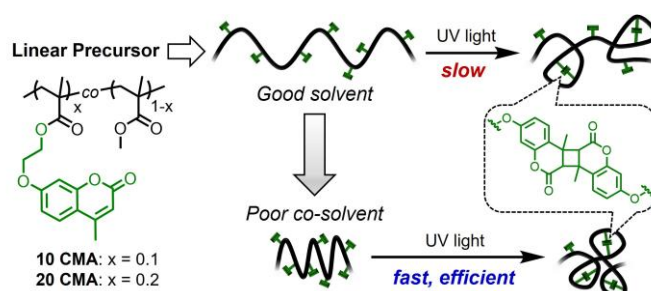


**Fig. 1.** Intrachain crosslinking of methyl methacrylate-based copolymers through the photoinduced dimerization of pendent coumarin units. The addition of poor solvents resulted in faster and more efficient crosslinking due to more compacted polymer chain dimensions. The [2+2] coumarin cycloaddition typically yields a mixture of isomers. For simplicity, only the head-to-tail dimer is shown.

solvents.<sup>23</sup> Inspired by this work, we wished to further explore the potential of exploiting solvent quality to enhance intramolecular crosslinking in organic solvents and elucidate the relationship between solvent-induced polymer chain compaction and crosslinking kinetics.

Specifically, we studied SCNP formation of coumarin-containing poly(methyl methacrylate) (PMMA) through photoinduced [2+2] cycloaddition<sup>24</sup> in solvents of varying polymer solvation quality (Figure 1). The coumarin chromophore allowed reaction monitoring and detailed kinetic analysis *via* UV-vis spectroscopy. By comparing with the reaction rates of model small molecules and monitoring the intramolecular crosslinking of the analogous polymers by static light scattering (SLS) and size-exclusion chromatography (SEC), we were able to gain insight into the role of solvophobic interactions on the kinetics and efficiency of the crosslinking reaction. We believe that such straightforward solvent control over chain conformation and reaction kinetics is not only highly desirable and easily implementable in SCNP synthesis, but also generally applicable to the design of other reactions involving macromolecules.

<sup>a</sup> George & Josephine Butler Polymer Research Laboratory, Center for Macromolecular Science & Engineering, Department of Chemistry, University of Florida, Gainesville, FL 32611, USA.

<sup>b</sup> Faculty of Materials Science and Engineering, South China University of Technology, Guangzhou 510640, People's Republic of China

\*Electronic Supplementary Information (ESI) available: Additional figures, procedures, and characterization data. See DOI: 10.1039/x0xx00000x

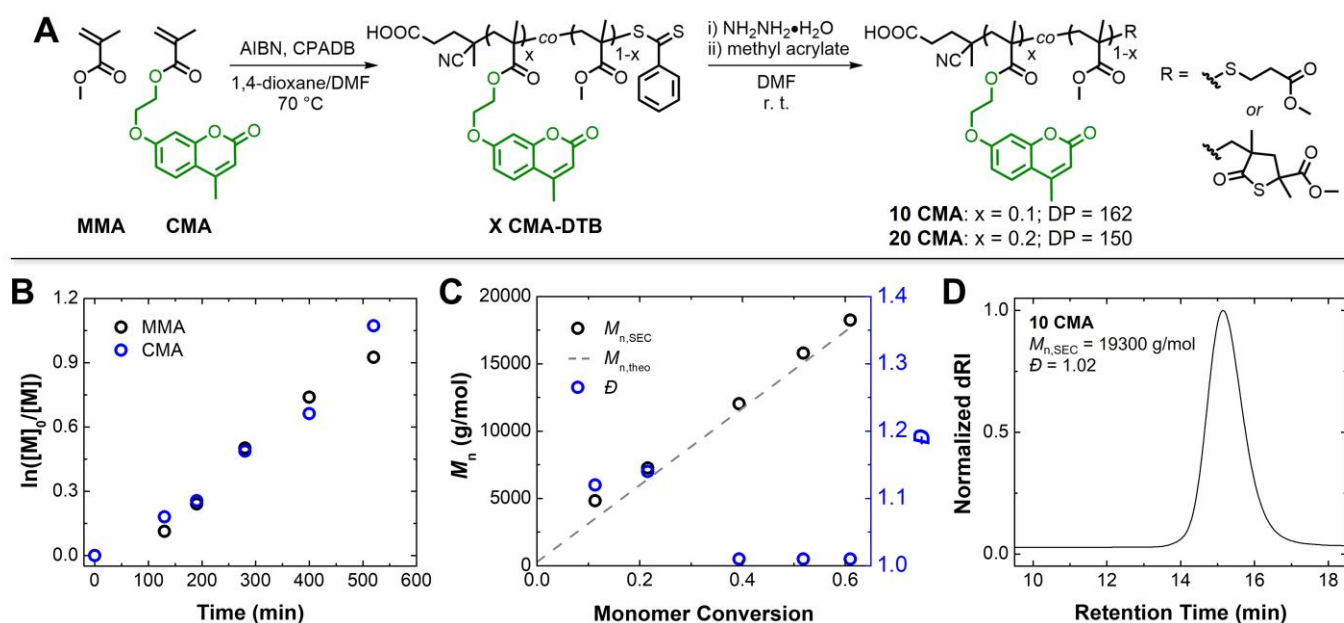


**Fig. 2** Synthesis of 10 CMA and 20 CMA. (A) Reversible addition-fragmentation chain transfer (RAFT) copolymerization of methyl methacrylate (MMA) and a 4-methylcoumarin methacrylate derivative (CMA) with 4-cyanopentanoic acid dithiobenzoate (CPADB) followed by end-group removal afforded 10 CMA and 20 CMA with similar degrees of polymerization. (B) Pseudo-first-order kinetic plot for MMA and CMA from the synthesis of 10 CMA. (C) Evolution of number-average molecular weight ( $M_n$ ) and dispersity ( $\bar{D}$ ) with monomer conversion for 10 CMA-DTB (i.e., 10 CMA containing the RAFT agent-derived end groups). (D) Size-exclusion chromatogram of 10 CMA (i.e., after end-group removal).  $M_n$  and  $\bar{D}$  values were obtained by size-exclusion chromatography (SEC) in *N,N*-dimethylacetamide coupled with multi-angle light scattering detection.

## Results and Discussion

### Polymer Synthesis

To study the influence of copolymer composition and solvent quality on the photoinduced intrachain crosslinking reaction, we synthesized PMMA-based copolymers with 10 and 20 mol% coumarin crosslinker content, denoted here as 10 CMA and 20 CMA, respectively. Both copolymers were synthesized by reversible addition-fragmentation chain transfer (RAFT) copolymerization (Figure 2). This reversible-deactivation radical polymerization technique was employed to obtain polymers with narrow molecular weight distributions, a prerequisite for obtaining uniform SCNPs.<sup>25</sup> Specifically, methyl methacrylate was copolymerized with a 4-methylcoumarin methacrylate derivative (CMA) using 4-cyanopentanoic acid dithiobenzoate (CPADB) as the RAFT agent (Figure 2A). Analysis of the polymerization kinetics revealed similar reaction rates for both monomers, consistent with statistical incorporation (Figure 2B). The unimodal shift to shorter elution times of the SEC signal of polymerization aliquots (Figure S1) and the agreement of number-average molecular weight ( $M_n$ ) with the theoretical values (Figure 2C) indicated a well-controlled polymerization. To avoid cross-reactivity of the photoactive dithiobenzoate moiety during the anticipated photoinduced crosslinking, we removed the RAFT agent-derived  $\omega$ -end group *via* aminolysis with hydrazine<sup>26</sup> followed

by thia-Michael addition with methyl acrylate.<sup>27</sup> To ensure the stability of the coumarin scaffold during this reaction, we conducted control experiments with 7-hydroxy-4-methylcoumarin, showing no change of the coumarin moiety upon exposure to excess hydrazine and thiols (Figure S2). While the thia-Michael product is the most probable polymer chain end after this reaction sequence,<sup>27,28</sup> we cannot exclude the possibility that some chains could be terminated by a thiolactone formed between the intermediate thiolate chain end and the penultimate methyl ester unit.<sup>29</sup> However, both chain end types should be stable towards UV irradiation at wavelengths above 350 nm and thus should not have interfered with the subsequent photo-crosslinking. <sup>1</sup>H NMR spectroscopy verified complete dithiobenzoate removal from the copolymers while maintaining all coumarin resonances (Figures S3 and S4). Finally, after purification *via* precipitation, we obtained 10 CMA and 20 CMA with dispersities ( $\bar{D}$ ) below 1.05 and an  $M_n$  of 19300 ( $DP_n = 162$ ) and 20700 g/mol ( $DP_n = 150$ ), respectively (Figures 2D and S4). The final coumarin content in the copolymers was determined by <sup>1</sup>H NMR spectroscopy by comparing the coumarin resonances with the PMMA methyl ester signal (Figures S3 and S4). Matching the initial feed ratios, we found 10.3 and 20.9 mol% coumarin incorporation for 10 CMA and 20 CMA, respectively.

### Solvent selection

With the copolymers in hand (Table S1), we sought to investigate the effect of solvent on precursor chain compaction and photo-crosslinking. Specifically, we envisioned DCM serving as a good solvent for the copolymer and 1/1 (v/v) solvent mixtures of dichloromethane (DCM) with methanol (MeOH) or hexanes (Hx) for the poor solvent conditions. To evaluate the solvent quality for the copolymers prior to the crosslinking experiments, we determined the second osmotic virial coefficient ( $B$ ) of a high-molecular-weight 20 CMA model copolymer *via* SLS and Zimm analysis (Figure S5).  $B$  relates to the concentration dependence of the scattering, whereby  $B$  decreases to zero for theta solvents and becomes negative for poor solvents.<sup>30</sup> The 20 CMA model copolymer was synthesized *via* RAFT copolymerization according to our protocol; however, we raised the molecular weight of the model copolymer ( $M_{n,SEC} = 63000$  g/mol) compared to the SCNP precursor copolymer to increase the scattering intensity and improve the sensitivity of the SLS analysis. In DCM,  $B$  was  $1.1 \times 10^{-6}$  mol $\cdot$ dm $^3$ /g $^2$  and decreased by almost two orders of magnitude to  $5.7 \times 10^{-8}$  mol $\cdot$ dm $^3$ /g $^2$  in 1/1 DCM/MeOH. We attempted SLS in 1/1 DCM/Hx; however, the poor solubility of the model copolymer in that solvent mixture prohibited analysis at concentrations above 5 mg/mL. These results suggested the solvent quality for the model copolymer decreased substantially from DCM > DCM/MeOH > DCM/Hx.

### Chain compaction

We next investigated the degree of chain compaction upon photo-crosslinking of 10 CMA and 20 CMA SCNP precursors in DCM, DCM/MeOH, and DCM/Hx (Figure 3A). The copolymers were irradiated with UV light ( $\lambda_{max} = 365$  nm) at low concentration (0.1 mg/mL), and the products were analyzed by SEC to verify a reduction in hydrodynamic volume<sup>31</sup> (*i.e.*, chain compaction) upon crosslinking and by UV-vis spectroscopy to determine the coumarin conversion. SEC bears critical limitations in determining absolute SCNP size,<sup>32</sup> particularly if additional enthalpic interactions between polymer and column material evolve due to changes of the polymer composition upon crosslinking.<sup>33</sup> Here, chain compaction occurred without introducing an external crosslinker, and thus, assuming only minimal changes in polymer polarity upon coumarin dimerization, the chemical composition should remain relatively constant within the respective copolymer series. All irradiated copolymers exhibited increased elution times compared to their linear parent polymer, indicating successful chain compaction (Figures 3B and S6). Under poor solvent conditions, the photo-crosslinking resulted in more pronounced chain compactations, with DCM/Hx causing the most dramatic size reduction, in line with the solvation trends observed by SLS.

To compare the two different copolymer compositions, we defined a measure for the relative size reduction by dividing the SCNP peak molecular weight ( $M_{p,SCNP}$ ) by the peak molecular weight of the parent copolymers ( $M_{p,PP}$ ; Figure 3C). Across all solvent conditions, 20 CMA provided more compacted SCNPs compared to 10 CMA, which could be

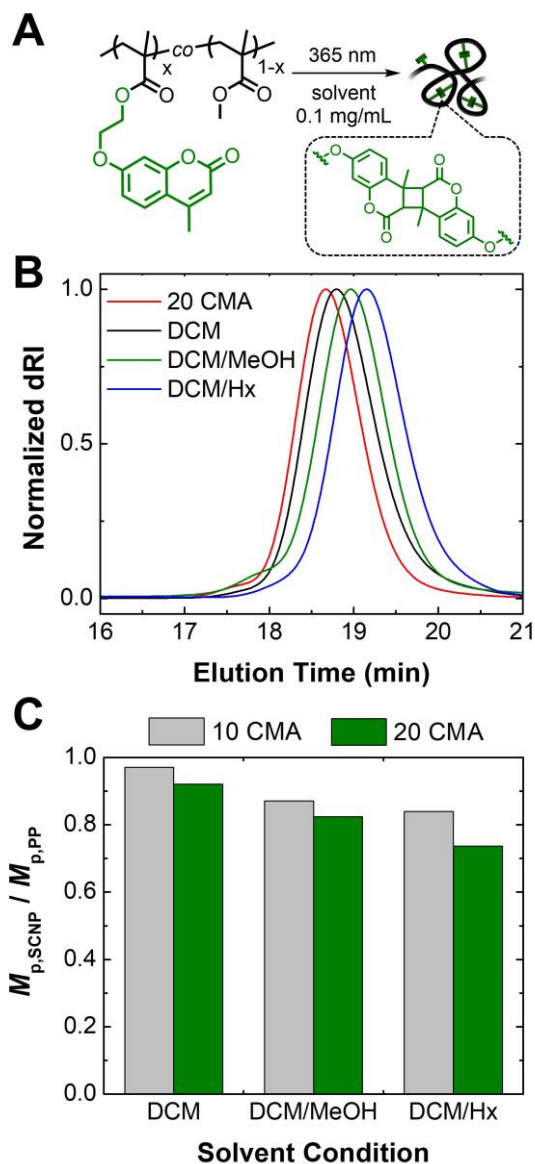


**Fig. 3.** Solvophobicity effects on the chain compaction. (A) Reaction scheme for SCNP formation using UV light ( $\lambda_{max} = 365$  nm). (B) Representative SEC traces of crosslinked SCNPs formed in different solvent systems from linear 20 CMA. SEC was conducted in tetrahydrofuran (THF). Coumarin conversions for the 20 CMA SCNPs: 69% (DCM), 86% (DCM/MeOH), 79% (DCM/Hx). (C) Bar graph comparing the relative chain compactations between copolymer series. Peak molecular weight ( $M_p$ ) of SCNP and parent polymer (PP) were determined *via* conventional calibration with polystyrene standards in THF. Coumarin conversions for 10 CMA SCNPs: 54% (DCM), 78% (DCM/MeOH), 66% (DCM/Hx).

attributed to the higher crosslinking density of 20 CMA-derived SCNPs resulting in denser particles. This result is in line with the findings of Berda and coworkers for disulfide-containing SCNPs.<sup>34</sup>

The final efficiency of coumarin photodimerization strongly depended on the solvent system (Figure S7, Table S2). After 8.5 h irradiation, the highest conversions were observed in DCM/MeOH, followed by DCM/Hx, and finally DCM. Notably, despite lower coumarin conversions, crosslinking in DCM/Hx still afforded more compacted particles compared to DCM/MeOH. In other words, the pre-compacted chains in the solvent with the lowest polymer solvation (*i.e.*, DCM/Hx)

facilitated an arrangement of intrachain crosslinks that resulted in smaller nanoparticles.

result suggests that in addition to the solvent polarity-induced rate increase, polymer-selective solvophobic interactions increase the reaction rate in the macromolecular system.

Critically, in DCM/Hx, 10 CMA and 20 CMA exhibited a 1.5

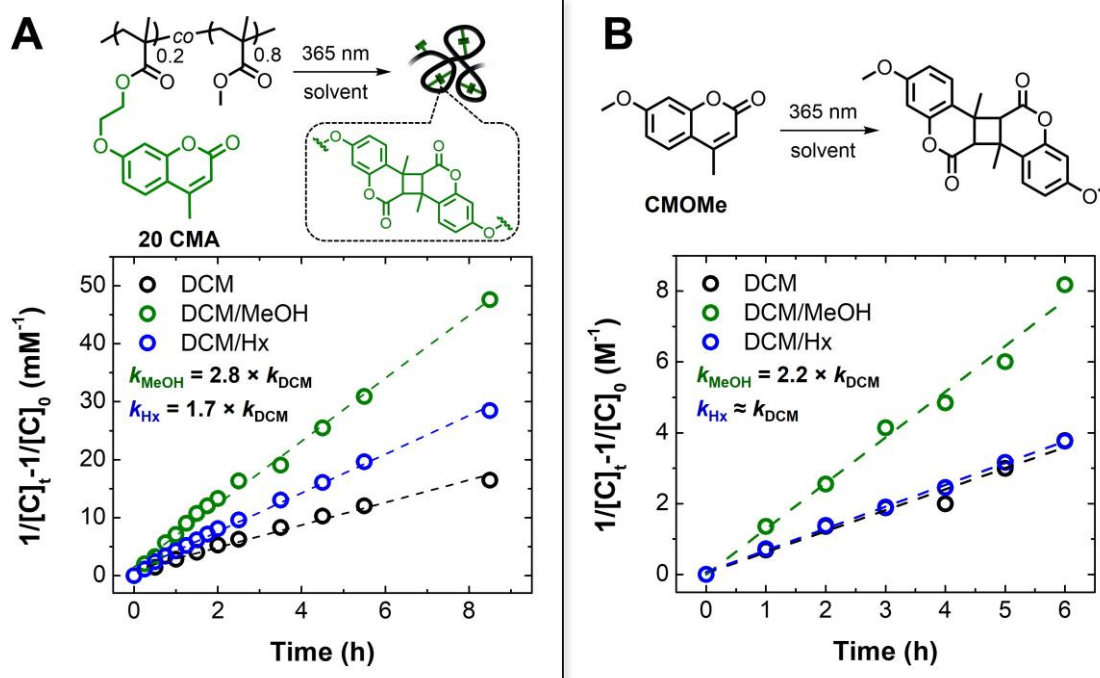


**Fig. 4.** Photoinduced [2+2] cycloaddition kinetics for a polymeric (A) and a small molecule (B) coumarin system in different solvents. (A) Representative second-order rate analysis for the photo-crosslinking of (A) 20 CMA ( $R^2 = 0.98$  (DCM), 0.99 (DCM/MeOH), 0.99 (DCM/Hx)) and (B) 7-methoxy-4-methylcoumarin (CMOMe;  $R^2 = 0.97$  (DCM), 0.99 (DCM/MeOH), 0.99 (DCM/Hx)).

### Crosslinking kinetics

Intrigued by solvent effects on coumarin conversion, we investigated the crosslinking kinetics of SCNP formation with 10 CMA and 20 CMA in DCM, DCM/MeOH, and DCM/Hx. Photodimerization conversion was calculated from the UV absorbance value at 319 nm and the molar extinction coefficient of the coumarin moieties in the respective solvent (Figures S8–S10 and Table S3). Furthermore, we subjected the non-polymeric coumarin model compound 7-methoxy-4-methylcoumarin (CMOMe) to UV irradiation under the same solvent conditions as the copolymers (Table S4) to distinguish between contributions from coumarin-solvent and polymer-solvent interactions. The data were fit to a linearized second-order rate law (equation 1):

$$\frac{1}{[C]_t} - \frac{1}{[C]_0} = kt \quad (1)$$

where  $[C]$  as the coumarin concentration,  $k$  is the solvent-dependent rate constant, and  $t$  is the UV exposure time. The kinetic analysis revealed the highest dimerization rate constant in DCM/MeOH for all the coumarin systems (Figures 4, S11, and Table S5). This can be attributed to the polar nature of MeOH, which has been shown to increase the quantum yield and accelerate the photoinduced dimerization of coumarins.<sup>35,36</sup> However, the copolymers series showed a more pronounced rate increase after switching from DCM to DCM/MeOH than the analogous small molecule system. This

and 1.7-fold rate increase compared to the dimerization rate in DCM. Conversely, no significant difference between DCM and DCM/Hx could be observed for the photodimerization of the small molecule analog. This comparison suggests the addition of Hx as a poor solvent selectively accelerates the reaction rate in polymeric systems. Considering the trends for polymer solvation and SCNP compaction measured by SLS and SEC, we believe that this rate increase can be attributed to a chain compaction of the linear precursor, arranging the coumarin moieties in closer proximity and raising the reaction rate through a polymer-selective solvophobic effect.<sup>37</sup>

### Conclusions

We studied solvent effects on SCNP synthesis by investigating chain compaction and photo-crosslinking kinetics of coumarin-containing methacrylate copolymers. Comparison with a molecular coumarin system revealed that solvophobic interactions involving the polymer chain of the linear SCNP precursors promoted the formation of more compacted SNCPs and substantially increased the crosslinking rate constants.<sup>37</sup>

This study showcases the potential of the solvophobic effect to drive pre-compaction and intrachain crosslinking kinetics in SCNP synthesis. Conceptually, this strategy mimics disulfide bridge formation in proteins, where covalent bond formation is preceded by polypeptide folding.<sup>38</sup> We believe that such solvophobicity-controlled crosslinking in organic

solvents opens new opportunities for future advancements in SCNP morphology<sup>22</sup> or synthesis,<sup>16</sup> and can be further applied to other macromolecular materials comprised of copolymers.<sup>39</sup>

### Conflicts of interest

There are no conflicts to declare.

### Acknowledgements

This research was supported by the DoD (W911NF-17-1-0326) and the NSF (DMR-1904631).

### Notes and references

- R. Chen and E. B. Berda, *ACS Macro Lett.*, 2020, **9**, 1836–1843.
- E. Huerta, P. J. Stals, E. W. Meijer and A. R. Palmans, *Angew. Chem. Int. Ed.*, 2013, **52**, 2906–2910.
- I. Perez-Baena, F. Barroso-Bujans, U. Gasser, A. Arbe, A. J. Moreno, J. Colmenero and J. A. Pomposo, *ACS Macro Lett.*, 2013, **2**, 775–779.
- J. Chen, E. S. Garcia and S. C. Zimmerman, *Acc. Chem. Res.*, 2020, **53**, 1244–1256.
- H. Rothfuss, N. D. Knofel, P. W. Roesky and C. Barner-Kowollik, *J. Am. Chem. Soc.*, 2018, **140**, 5875–5881.
- A. Sanchez-Sanchez, S. Akbari, A. Etxeberria, A. Arbe, U. Gasser, A. J. Moreno, J. Colmenero and J. A. Pomposo, *ACS Macro Lett.*, 2013, **2**, 491–495.
- J. Chen, K. Li, J. S. L. Shon and S. C. Zimmerman, *J. Am. Chem. Soc.*, 2020, **142**, 4565–4569.
- A. P. P. Kroger and J. M. J. Paulusse, *J. Control. Release*, 2018, **286**, 326–347.
- O. Galant, S. Bae, M. N. Silberstein and C. E. Diesendruck, *Adv. Funct. Mater.*, 2019, **30**, 1901806.
- A. Arbe, J. A. Pomposo, I. Asenjo-Sanz, D. Bhowmik, O. Ivanova, J. Kohlbrecher and J. Colmenero, *Macromolecules*, 2016, **49**, 2354–2364.
- M. E. Mackay, T. T. Dao, A. Tuteja, D. L. Ho, B. van Horn, H. C. Kim and C. J. Hawker, *Nat. Mater.*, 2003, **2**, 762–766.
- H. S. Wang, A. Khan, Y. Choe, J. Huh and J. Bang, *Macromolecules*, 2017, **50**, 5025–5032.
- Y. Zheng, H. Cao, B. Newland, Y. Dong, A. Pandit and W. Wang, *J. Am. Chem. Soc.*, 2011, **133**, 13130–13137.
- A. M. Hanlon, R. Chen, K. J. Rodriguez, C. Willis, J. G. Dickinson, M. Cashman and E. B. Berda, *Macromolecules*, 2017, **50**, 2996–3003.
- H. Frisch, J. P. Menzel, F. R. Bloesser, D. E. Marschner, K. Mundsinger and C. Barner-Kowollik, *J. Am. Chem. Soc.*, 2018, **140**, 9551–9557.
- O. Galant, H. B. Donmez, C. Barner-Kowollik and C. E. Diesendruck, *Angew. Chem. Int. Ed.*, 2021, **60**, 2042–2046.
- Y. Hirai, T. Terashima, M. Takenaka and M. Sawamoto, *Macromolecules*, 2016, **49**, 5084–5091.
- M. Matsumoto, T. Terashima, K. Matsumoto, M. Takenaka and M. Sawamoto, *J. Am. Chem. Soc.*, 2017, **139**, 7164–7167.
- J. W. Liu, M. E. Mackay and P. M. Duxbury, *Macromolecules*, 2009, **42**, 8534–8542.
- H. Rabbal, P. Breier and J.-U. Sommer, *Macromolecules*, 2017, **50**, 7410–7418.
- F. Lo Verso, J. A. Pomposo, J. Colmenero and A. J. Moreno, *Soft Matter*, 2015, **11**, 1369–1375.
- C. H. Liu, L. D. Dugas, J. I. Bowman, T. Chidanguro, R. F. Storey and Y. C. Simon, *Polym. Chem.*, 2020, **11**, 292–297.
- J. Engelke, B. T. Tuten, R. Schweins, H. Komber, L. Barner, L. Plüschke, C. Barner-Kowollik and A. Lederer, *Polym. Chem.*, 2020, **11**, 6559–6578.
- J. He, L. Tremblay, S. Lacelle and Y. Zhao, *Soft Matter*, 2011, **7**, 2380–2386.
- K. Parkatzidis, H. S. Wang, N. P. Truong and A. Anastasaki, *Chem*, 2020, **6**, 1575–1588.
- W. Shen, Q. Qiu, Y. Wang, M. Miao, B. Li, T. Zhang, A. Cao and Z. An, *Macromol. Rapid Commun.*, 2010, **31**, 1444–1448.
- V. Lima, X. Jiang, J. Brokken-Zijp, P. J. Schoenmakers, B. Klumperman and R. Van Der Linde, *J. Polym. Sci., Part A: Polym. Chem.*, 2005, **43**, 959–973.
- X.-P. Qiu and F. M. Winnik, *Macromol. Rapid Commun.*, 2006, **27**, 1648–1653.
- J. Xu, J. He, D. Fan, X. Wang and Y. Yang, *Macromolecules*, 2006, **39**, 8616–8624.
- P. C. Hiemenz and T. P. Lodge, *Polymer Chemistry*, CRC Press, Boca Raton, FL, 2nd edn., 2007.
- A. Latorre-Sánchez, A. Alegría, F. Lo Verso, A. J. Moreno, A. Arbe, J. Colmenero and J. A. Pomposo, *Part. Part. Syst. Charact.*, 2016, **33**, 373–381.
- J. Engelke, J. Brandt, C. Barner-Kowollik and A. Lederer, *Polym. Chem.*, 2019, **10**, 3410–3425.
- E. Blasco, B. T. Tuten, H. Frisch, A. Lederer and C. Barner-Kowollik, *Polym. Chem.*, 2017, **8**, 5845–5851.
- B. T. Tuten, D. Chao, C. K. Lyon and E. B. Berda, *Polym. Chem.*, 2012, **3**, 3068–3071.
- T. Wolff and H. Gerner, *Phys. Chem. Chem. Phys.*, 2004, **6**, 368–376.
- Coumarin also showed the highest molar extinction coefficient in the solvent mixture with methanol (Figure S10).
- L. Yang, C. Adam and S. L. Cockroft, *J. Am. Chem. Soc.*, 2015, **137**, 10084–10087.
- M. Qin, W. Wang and D. Thirumalai, *Proceedings of the National Academy of Sciences*, 2015, **112**, 11241.
- J. J. Lessard, G. M. Scheutz, S. H. Sung, K. A. Lantz, T. H. Epps and B. S. Sumerlin, *J. Am. Chem. Soc.*, 2020, **142**, 283–289.